Ore Geology Reviews 64 (2015) 736–746

Contents lists available at ScienceDirect

Ore Geology Reviews

journal homepage: www.elsevier.com/locate/oregeorev

Effects of fluorine on the solubilities of Nb, Ta, Zr and Hf minerals in highly fluxed water-saturated haplogranitic melts

Abdullah A. Aseri [a,b,c,*], Robert L. Linnen [b,**], Xu Dong Che [d], Yves Thibault [e], François Holtz [f]

[a] Department of Earth and Environmental Sciences, University of Waterloo, Waterloo, Ontario N2L 3G1, Canada
[b] Department of Earth Sciences, University of Western Ontario, London, Ontario N5A 5B7, Canada
[c] King Abdul Aziz University, Jeddah, Saudi Arabia
[d] State Key Laboratory for Mineral Deposits Research, School of Earth Sciences and Engineering, Nanjing University, Nanjing 210093, China
[e] CANMET-MMSL, Natural Resources Canada, 555 Booth Street, Ottawa, Ontario K1A 0G1, Canada
[f] Institut für Mineralogie, Leibniz Universität Hannover, Callinstraße 3, D-30167 Hannover, Germany

ARTICLE INFO

Article history:
Received 16 June 2013
Received in revised form 13 January 2014
Accepted 27 February 2014
Available online 19 March 20147

Keywords:
Fluorine
Pegmatite
Flux-rich
Solubility
Columbite
Tantalite
Zircon
Hafnon

ABSTRACT

The effect of fluorine on the solubilities of Mn-columbite ($MnNb_2O_6$), Mn-tantalite ($MnTa_2O_6$), zircon ($ZrSiO_4$) and hafnon ($HfSiO_4$) were determined in highly fluxed, water-saturated haplogranitic melts at 800 to 1000 °C and 2 kbar. The melt composition corresponds to the intersection of the granite minimum with the albite–orthoclase tieline ($Ab_{72}Or_{28}$) in the quartz–albite–orthoclase system (Q–Ab–Or), which is representative of a highly fluxed melt, from which high field strength element minerals may crystallize. The melt contains 1.7 wt.% P_2O_5, 1.05 wt.% Li_2O and 1.83 wt.% B_2O_3. The main purpose of this study is to examine the effect of F on columbite, tantalite, zircon and hafnon solubility for a melt with this composition. Up to 6 wt.% fluorine was added as AgF in order to keep the aluminum saturation index (ASI, molar Al/[Na + K]) of the melt constant. In an additional experiment F was added as AlF_3 to make a glass peraluminous. The nominal ASI of the melts are close to 1 for the minimum composition and approximately 1.32 in peraluminous glasses, but if Li is considered as an alkali, the molar ratio Al/[Na + K + Li] of the melts are alkaline (0.87) and subaluminous (1.09), respectively.

The molar solubility products [MnO] * [Nb_2O_5] and [MnO] * [Ta_2O_5] are nearly independent of the F content of the melt, at approximately 18.19 ± 1.2 and 43.65 ± 2.5 × 10^{-4} (mol^2/kg^2), respectively for the minimum composition. By contrast, there is a positive dependence of zircon and hafnon solubilities on the fluorine content in the minimum composition, which increases from 2.03 ± 0.03 × 10^{-4} (mol/kg) ZrO_2 and 4.04 ± 0.2 × 10^{-4} (mol/kg) HfO_2 for melts with 0 wt.% F to 3.81 ± 0.3 × 10^{-4} (mol/kg) ZrO_2 and 6.18 ± 0.04 × 10^{-4} (mol/kg) HfO_2 for melts with 8 wt.% F. Comparison of the data from this work and previous studies indicates that ASI of the melt seems to have a stronger effect than the contents of fluxing elements in the melt and the overall conclusion is that fluorine is less important (relative to melt compositions) than previously thought for the control on the behavior of high field strength elements in highly evolved granitic melts. Moreover, this study confirms that although Nb, Ta, Zr and Hf are all high field strength elements, Nb–Ta and Zr–Hf are complexed differently in the melt.

1. Introduction

Concentrations of trace elements in granitic melts change significantly as crystallization advances. The main factor that controls whether elements concentrate in the residual melt or disseminate in the major or accessory minerals is the compatibility of those elements between minerals and the melt, and the solubilities of accessory minerals. The latter are governed by temperature, pressure and the melt composition. Niobium, tantalum, zirconium and hafnium are high field strength elements (HFSE), and these elements do not substitute into most rock forming-minerals, thus they are concentrated in the silicate melts by fractional crystallization until the saturation of accessory phases such as columbite or zircon is reached. These elements are increasingly important to society. A few examples are the use of niobium in high-strength low alloy steel, tantalum in capacitors for wireless devices and touch screen technologies, and zirconium and hafnium both have applications to the nuclear industry (Linnen et al., 2014).

Rare element pegmatites are classified into two families, the LCT family is enriched in Li, Cs and Ta and the NYF family is enriched in Nb, Y and F (Černý et al., 2005). The LCT family is peraluminous, and is economically important because these pegmatites are exploited

* Corresponding author at: Department of Earth and Environmental Sciences, University of Waterloo, Waterloo, Ontario N2L 3G1, Canada.
** Corresponding author.
E-mail addresses: aaseri@uwo.ca (A.A. Aseri), rlinnen@uwo.ca (R.L. Linnen).

http://dx.doi.org/10.1016/j.oregeorev.2014.02.014
0169-1368/

for Li, Cs and Ta. The most common Nb–Ta mineral in this family is columbite–tantalite and the most common Zr–Hf mineral is zircon–hafnon. The NYF-family is more alkalic (London, 2008) and these pegmatites are generally not economic. Both families contain elevated amounts of fluxing elements such as H_2O, P, Li, B and F (Linnen and Cuney, 2005). Fluxing elements play an important role in magma evolution by causing significant changes in the melt structure, which affect melt properties such as viscosity and diffusivity (London, 2008). The controls of HFSE mineral saturation is a key to understanding pegmatite petrogenesis, even where the concentrations of HFSE in the melt may be low, e.g. Zr–Hf for zircon–hafnon saturation (e.g., Van Lichtervelde et al., 2007). Because Nb–Ta and Zr–Hf have similar charge and ionic radii, variations in Nb/Ta and Zr/Hf ratios are not expected, but Linnen and Keppler (1997) showed that the solubility of tantalite is higher than columbite and Linnen and Keppler (2002) determined that hafnon is more soluble than zircon in subaluminous granitic melts. In both cases these authors concluded that the low Nb/Ta and Zr/Hf ratios observed in highly evolved granites are the result of extreme fractional crystallization.

The two most important parameters that control the solubilities of columbite–-tantalite and zircon–-hafnon in granitic melts are temperature and melt composition (e.g., Bartels et al., 2010; Linnen and Keppler, 1997; Linnen and Keppler, 2002; Van Lichtervelde et al., 2010; Watson, 1979). Pressure has a relatively small effect (Chevychelov et al., 2010; Linnen and Keppler, 1997) and for melts with more than approximately 1 wt.% H_2O, the water content of the melt does not affect HFSE mineral solubility (Linnen, 2005). The LCT family of pegmatites are interpreted to have crystallized from melts that contained elevated concentrations of Li, B, P and F (London, 1987) consequently the roles of these compounds to pegmatite evolution has received considerable attention. Fluorine is particularly important because tantalum mineralization is commonly associated with fluorine-rich rocks (cf. Wise et al. 2012 and the references therein). Similarly in granitic systems Nb–Ta–W–Sn mineralization is commonly associated with Li–F–P-rich granites (e.g., Badanina et al., 2010; Breiter et al., 2007; Raimbault and Burnol, 1998).

However, the effect of fluorine on the solubilities of columbite–tantalite and zircon–hafnon in granitic melts is controversial. Keppler (1993) reported that the solubilities of columbite, tantalite and zircon increase with increasing F content in the melt. The enhancement of solubility was explained by increasing non-bridging oxygen (NBO) in the melts due to the reaction of F with Al to form AlF_6^{-3} complexes. By contrast, Baker et al. (2002) concluded that F has only a weak effect on the solubilities of zircon, Van Lichtervelde et al. (2010) also observed only a weak effect of F on tantalite and zircon solubility and similarly, Fiege et al (2011) concluded that F has no effect on the solubilities of tantalite and columbite in subaluminous haplogranitic melts. In order to resolve the conflicting results on the effect of fluorine on columbite–tantalite and zircon–hafnon solubilities a new experimental study was undertaken. Most of the experiments were carried out using a melt composition with an ASI (molar Al/[Na + K]) of 1.0, but a peraluminous melt composition was investigated to examine the F effect at a higher ASI value.

2. Methodology

2.1. Starting glasses

Melt inclusions in the pegmatites and granites that host Nb–Ta mineralization commonly have high concentrations of fluxing compounds (e.g., Badanina et al., 2010; Borisova et al., 2012; Thomas et al., 2000; Webster et al., 1997). It is also apparent that, although these pegmatites and granites are peraluminous, the HFSE mineralization may crystallize from a more alkaline melt (London, 2008; Thomas et al., 2011). Because fluxes shift the granite minimum composition away from the quartz apex, the starting glass was prepared to correspond to the composition where the 2 kbar water-saturated granite minimum lies on the albite–orthoclase tieline in the quartz–albite–orthoclase system ($Ab_{72}Or_{28}$; where the shift in granite minimum composition is due to the addition of P_2O_5, London et al, 1993). The highly fluxed haplogranite glass was prepared by mixing SiO_2, Al_2O_3, Na_2CO_3, K_2CO_3 with Li_3PO_4, and B_2O_3 and heated gradually to degas the CO_2. The mixture was loaded into a platinum crucible and placed in a furnace at 1200 °C for 24 h to produce a glass with 1.1 wt.% Li_2O, 1.7 wt.% P_2O_5 and 2.0 wt.% B_2O_3. After 24 h, the melt was quenched and the glass was crushed and ground into a fine powder in an agate mortar. To insure homogeneity, the glass was reheated and ground a second time. After the second melting small pieces of the glass were taken to be analyzed by electron microprobe (EMP) then the rest was ground into fine powder, which also was analyzed by ICP-MS.

In order to study the effect of fluorine on the solubility of Mn-columbite, Mn-tantalite, zircon and hafnon, three fluorine-rich glasses were prepared with approximately 2, 4, 6 wt.% F by adding AgF to the initial glass. The molar ASI (Al/[Na + K]) ratio and the molar ASI_{Li} (Al/[Na + K + Li]) ratio are almost constant in all experiments (about 1.05 and 0.87, respectively) and the only variable is the fluorine concentration. A fourth F-rich glass was prepared by adding AlF_3. This glass is nominally peraluminous and has a F content of 6 wt.%. The molar ASI (Al/[Na + K]) ratio and the molar ASI_{Li} (Al/[Na + K + Li]) ratio of peraluminous glass are 1.32 and 1.09, respectively. About 400 mg of the starting glass powder and variable amounts of AgF or AlF_3 were mixed and loaded in gold capsules (3 cm length and 5 mm o.d.) with 8 wt.% (32 mg) H_2O to be nearly water saturated. Capsules were then shut and sealed by arc welder and placed in rapid quench cold seal pressure vessels (CSPV) at 2 kbar and 800 °C for five days. Later, the fluorine-rich water saturated glasses were crushed and ground into fine powder.

2.2. Starting minerals

Synthetic Mn-columbite, Mn-tantalite, hafnon and natural zircon (from Miask, Ural) were used to conduct solubility experiments. These minerals are commonly associated with evolved granites and pegmatites except for hafnon.

Solubility experiments were prepared by gently mixing about 30 mg of fluorine-rich or fluorine-free powder and 3 mg of crystals of the investigated minerals. The mixture was loaded into a gold capsule (2 cm length and 3 mm o.d.) shut and sealed by an arc welder then placed in a drying oven at 110 °C. Before starting the experiments, capsules were weighed to ensure that there was no leakage, and then placed in autoclaves at 700 to 1000 °C and 2 kbar for two to five days. After five days, the experiments were quenched isobarically, and then small chips were taken and mounted in an epoxy puck to be analyzed by electron microprobe after polishing.

In order to study the effect of F on the solubilities of Mn-columbite, Mn-tantalite and hafnon at different ASI, three experiments were conducted at 800 °C and 2 kbar using AlF_3 as a fluorine source, following the same procedures described above. For the 0 and 6 wt.% F glass compositions additional experiments were conducted for columbite, tantalite, zircon and hafnon solubilities in order to study the effect of temperature on solubility. These experiments also provided the starting glasses for crystallization (reverse) experiments, where equilibrium is approached from an over-saturated melt. For the high temperature experiments about 70 mg hydrous glass and about 7 mg of crystals were loaded into 5 mm o.d. platinum capsules, then shut and sealed by an arc welder. The experiments were conducted in vertically mounted internally-heated pressure vessels at Leibniz University, Hannover, Germany at 1000 °C and 2 kbar for two days. About 50% of each experiment product was used for EMP analysis and the other 50% was used to conduct the reverse experiments.

Crystallization experiments were performed by using the glass products of the high temperature experiments. About 50 mg of glass was loaded into gold capsules and doped with about 3 mg of crystals in an attempt to prevent the nucleation of microcrystals. Capsules

were prepared using the procedures described above, then placed in CSPV for five days at 800 °C and 2 kbar. Later, small pieces of glass were taken to be analyzed by EMP.

2.3. Analytical techniques

All quenched experiments were weighed before opening to check for leaks. The experimental products were mounted in epoxy then polished. The concentrations of Li and B in the starting material were taken to be the same as the starting glass measured by inductively coupled plasma mass spectroscopy (ICP/MS). The concentration H_2O was estimated from the EMP analysis, but according to Linnen (2005), the effect of water on the solubilities of HFSE minerals is negligible for melts with greater than 3 wt.% H_2O. The major elements (except for Li, B and H_2O) of the starting glass, including their fluorine contents, were analyzed by a JEOL 733 microprobe at CANMET laboratory, Ottawa, Canada. Metal concentrations as well as major elements, were analyzed by a Cameca SX50 electron microprobe at the University of Toronto and a Cambax MBX microprobe at Carleton University, Ottawa, Canada.

The concentrations of Na, K, Al, Si, F and P were measured with a 15 kV accelerating voltage, 20 nA beam current, 10 s counting time for Al and Si, and 6 s for the rest of the elements and the beam diameter was 20 μm. The respective standards for the major elements were synthetic NaNb glass for Na, obsidian glass for Al, Si and K, synthetic CaF_2 glass for F and natural apatite for phosphorous. Trace element Nb, Ta, Zr and Hf concentrations were measured with 15 kV accelerating voltage, 60 nA beam current, counting time was between 40 and 60 s, and the beam diameter was 5 μm. The standards for the trace element analysis were synthetic NaNb glass for Nb, Ta metal for Ta, synthetic $ZrSiO_4$ for Zr and synthetic $HfSiO_4$ for Hf. Oxygen was calculated by cation stoichiometry and included in the matrix correction, and oxygen equivalent from F was subtracted in the matrix correction. The method of matrix correction was ZAF or Phi–Rho–Z calculations, and the mass absorption coefficient data set was CITZMU.

The Li and B contents in the starting powder, as well as the contents of the other major elements, were measured by inductively coupled plasma mass spectroscopy (ICP/MS) at ACTLABS facilities. For Li and B, glasses underwent a sodium peroxide fusion, followed by sintering at 650 °C in a muffle furnace and then dissolved in a solution of 5% nitric acid before ICP-MS analysis. The rest of the elements were measured using lithium metaborate/tetraborate fusion-ICP-MS method. In this method, the fused sample is diluted and analyzed by a Perkin Elmer Sciex ELAN 6000, 6100 or 9000 ICP-MS. The Li and B concentrations in the starting glasses with 0, 2, 4, 6 and 8 wt.% F were obtained by femtosecond laser-ablation inductively coupled plasma/mass spectroscopy (LA-ICP/MS) at the University of Windsor, Canada. The LA-ICP/MS analysis was acquired using 100 Hz repetition rate, 30.0 μJ energy after 2.5 mm pinhole, 21 μm beam width and using 10× reflective lens. The standard that was used in this analysis was NIST 610 and Si concentrations in the starting glasses, obtained by EMP, were used as an internal standard.

3. Results

The compositions of the starting glasses are given in Table 1. All solubility experiment products were glasses and crystals of investigated minerals and no other phases were observed. Careful analysis was conducted to determine the concentrations of major and trace elements in all glasses. Some major elements such as Na and F are difficult to analyze by EMP because they tend to diffuse away from the analyzed area during analysis. The starting glasses as well as some of the run glasses were analyzed by EMP at the CANMET laboratory in Ottawa for both major and trace elements. The CANMET results are similar to those obtained by ICP/MS, shows very similar concentrations of major elements (Na in particular) and the F concentrations are similar to values anticipated from glass synthesis. Therefore, these values are preferred and the major element contents in the run glasses are assumed to be the same as their concentration in the starting glasses and they are given in Table 1. The concentrations Nb, Ta, Zr, Hf and Mn were analyzed by electron microprobe and the results are given in Tables 2, 3, 4 and 5. Generally, the molar ratios of Mn/Nb and Mn/Ta in the glasses are close to the stoichiometric values of Mn-columbite and Mn-tantalite (Tables 2 and 3), which supports the interpretation that these are equilibrium values (Fiege et al., 2011). The dissolution reactions of these experiments can be written as molar solubility products, as discussed by Linnen and Keppler (1997), Linnen and Cuney (2005) and Bartels et al. (2010).

$$MnNb_2O_6{}^{crystal} = MnO^{melt} + Nb_2O_5{}^{melt}$$

$$MnTa_2O_6{}^{crystal} = MnO^{melt} + Ta_2O_5{}^{melt}.$$

The results of the dissolution reactions can be expressed in terms of solubility products

$$K_{Sp}^{MnNb}\left(mol^2/kg^2\right) = X\ (MnO)\ (mol/kg)\ .\ X\ (Nb_2O_5)\ (mol/kg)$$

Table 1
Starting glass compositions.

	D.gls	0.gls	2-gls	4-gls	6-gls	8-gls	gls*
SiO_2	64.01	57.45 (0.95)	56.17 (0.71)	54.68 (0.93)	53.61 (0.92)	51.20 (0.27)	52.82 (0.45)
Al_2O_3	18.73	16.98 (0.29)	16.73 (0.18)	16.31 (0.28)	15.96 (0.28)	15.14 (0.12)	18.83 (0.15)
Na_2O	7.76	7.25 (0.33)	7.06 (0.20)	6.97 (0.33)	6.37 (0.15)	6.32 (0.08)	6.35 (0.09)
K_2O	4.41	3.95 (0.11)	3.89 (0.09)	3.75 (0.11)	3.68 (0.50)	3.33 (0.04)	3.57 (0.03)
Li_2O^{**}	1.05	0.98	0.75	0.80	0.75	0.80	0.85
Ag_2O	–	–	0.53 (0.11)	2.04 (0.18)	1.64 (0.13)	6.00 (0.15)	–
P_2O_5	1.72	1.59 (0.17)	1.63 (0.17)	1.62 (0.17)	2.07 (0.21)	2.31 (0.09)	1.39 (0.06)
F	–	–	2.14 (0.14)	4.32 (0.18)	5.73 (0.09)	7.78 (0.11)	4.71 (0.10)
$B_2O_3^{**}$	1.83	1.28	1.17	0.79	1.15	1.15	1.20
$H_2O^{\approx}$	0	10.52	9.93	8.53 (0.51)	9.03 (0.54)	5.95 (0.2)	10.47 (0.42)
ASI (EA)	1.06 (−0.15)	1.05 (−0.15)	1.06 (−0.17)	1.05 (−0.15)	1.10 (−0.29)	1.08 (−0.22)	1.32 (−0.88)
ASI_{Li} (EA_{Li})	0.89 (0.47)	0.87 (0.50)	0.91 (0.33)	0.89 (0.38)	0.94 (0.21)	0.90 (0.31)	1.09 (−0.32)
ASI_{eff} (EA_{Li+P})	0.94 (0.22)	0.93 (0.28)	0.97 (0.10)	0.96 (0.15)	1.02 (−0.09)	1.00 (−0.02)	1.04 (−0.12)
2 F = O	–	–	−0.90	−1.82	−2.41	−3.27	−1.98
Total	99.52	100	99.1	98.18	97.59	96.73	98.02

Microprobe analysis of the starting glasses. Oxide values in parentheses represent 2σ standard deviation. Li^{**} and B^{**} contents were determined in the dry starting glass by ICP/MS. In hydrous starting glasses, Li and B values were obtained by LA-ICP/MS. $H_2O^{\approx}$ content was estimated by taking the difference of the total oxides to 100%. D.gls: anhydrous starting glass; 0.gls: hydrous starting glass; 2-gls to 8-gls: starting glasses contain variable F concentration; gls*: peraluminous glass where F was added as AlF_3. ASI is the molar ratio of Al / (Na + K); EA is the molar of Na + K–Al per kilogram; ASI_{Li} is the molar ratio of Al / (Na + K + Li); EA_{Li} is the molar of Na + K + Li–Al per kilogram; ASI_{eff} is the molar ratio of (Al ± P) / (Na + K + Li); and EA_{Li+P} is the molar Na + K + Li–Al ± P per kilogram (see the text for more information about P role).

Table 2
Mn-columbite solubility.

Experiments	T (C°)	P kbar	Duration (days)	ASI	EA	ASI_{Li}	EA_{Li}	ASI_{eff}	EA_{Li+P}	F wt.%	Ag_2O wt.%	MnO wt.%	Nb_2O_5 wt.%	Mn/Nb	$logK_{Sp}^{MnNb}$ $_{mol^{22}/kg}$
SO.46	700	2	5	1.10	−0.29	0.95	0.17	1.03	−0.13	6	0.0 (0.1)	0.22 (0.01)	0.49 (0.02)	0.84 (0.05)	−3.24 (0.02)
Nb1	800	2	5	1.05	−0.15	0.83	0.68	0.88	0.45	0	0.0	0.35 (0.02)	1.04 (0.03)	0.63 (0.05)	−2.72 (0.02)
Nb2	800	2	5	1.06	−0.17	0.86	−0.51	0.92	0.27	2	0.5 (0.11)	0.35 (0.03)	1.03 (0.06)	0.64 (0.06)	−2.72 (0.06)
Nb3	800	2	5	1.05	−0.15	0.85	0.55	0.91	0.32	4	2.0 (0.2)	0.33 (0.03)	0.99 (0.03)	0.63 (0.06)	−2.75 (0.06)
Nb4	800	2	5	1.10	−0.29	0.89	0.38	0.97	0.08	6	1.6 (0.13)	0.33 (0.04)	0.93 (0.15)	0.66 (0.08)	−2.79 (0.08)
SO.34	800	2	5	1.32	−0.88	1.07	−0.24	1.01	−0.04	6	0.0	0.15 (0.03)	0.39 (0.04)	0.73 (0.16)	−4.14 (0.04)
$SO.42^R$	800	2	5	1.05	−0.15	0.83	0.67	0.88	0.44	0	0.0	0.33 (0.02)	0.86 (0.03)	0.72 (0.08)	−2.81 (0.02)
$SO.38^R$	800	2	5	1.10	−0.29	0.89	0.36	1.01	0.07	6	bdt	0.31 (0.03)	0.75 (0.03)	0.77 (0.09)	−2.91 (0.03)
SO.1	1000	2	2	1.05	−0.15	0.76	0.99	0.81	0.77	0	0.0	0.95 (0.03)	3.19 (0.04)	0.56 (0.02)	−1.79 (0.01)
SO.5	1000	2	2	1.10	−0.29	0.81	0.69	0.89	0.40	6	0.2 (0.02)	0.97 (0.01)	3.28 (0.04)	0.55 (0.01)	−1.77 (0.01)

Microprobe analysis of Mn-columbite solubility. Values in parentheses represent 2σ standard deviation. R: reverse experiments. bdt: below detection limit. ASI is the molar ratio of Al/(Na + K); EA is the molar Na + K–Al per kilogram; ASI_{Li} is the molar ratio of Al/(Na + K + Li + 2 ∗ Mn); EA_{Li} is the molar Na + K + Li + 2 ∗ Mn–Al per kilogram; ASI_{eff} is the molar ratio of (Al ± P)/(Na + K + Li + 2*Mn); and EA_{Li+P} is the molar Na + K + Li + 2 ∗ Mn–Al ± P per kilogram (see the text for more information about P role).

$$K_{sp}^{MnTa}\left(mol^2/kg^2\right) = X\ (MnO)\ (mol/kg)\ .\ X\ (Ta_2O_5)\ (mol/kg)$$

where X represents the molar concentration of MnO, Nb_2O_5 and Ta_2O_5 in the melt.

Experiments that were carried out at 1000 °C also show stoichiometric values. The results of these experiments show that Mn-tantalite is more soluble than Mn-columbite at the same conditions which are in agreement with Keppler (1993), Linnen and Keppler (1997), Bartels et al. (2010) and Fiege et al. (2011). Very small crystals of Mn-columbite (SO.42R) and Mn-tantalite (SO.43R) nucleated during the reverse experiments at 800 °C and as such might affect EMP analysis. However, clean areas were found around large seed crystals, and these areas were used for EMP analysis (Fig. 1). One problem is that the average Mn/Nb ratio obtained from experiments conducted at 700 °C is 0.84 which is greater than the stoichiometric value of 0.50, whereas Mn/Ta for the 700 °C experiment has an average ratio of 0.28. These nonstoichiometric values could be due to slower diffusivity of Nb and Ta relative to Mn, which is more problematic at lower temperature. However, the values of the solubility products at 700 °C are consistent with those extrapolated from higher temperatures (see below); therefore, we interpret that these are close to equilibrium solubilities, and at worst represent minimum values.

The dissolution reactions of zircon and hafnon are:

$$ZrSiO_4{}^{crystal} = ZrO_2{}^{melt} + SiO_2{}^{melt}$$

$$HfSiO_4{}^{crystal} = HfO_2{}^{melt} + SiO_2{}^{melt}.$$

The equilibrium constant of zircon and hafnon dissolution reaction can be written as

$$K_{ZrSiO4} = \left(a_{ZrO2}^{melt} \cdot a_{SiO2}^{melt}\right)/a_{ZrSiO4}^{crystal}$$

$$K_{HfSiO4} = \left(a_{Hf\,O2}^{melt} \cdot a_{SiO2}^{melt}\right)/a_{Hf\,SiO4}^{crystal}$$

where α is the activities of $ZrSiO_4$, $HfSiO_4$, ZrO_2, HfO_2 and SiO_2. However, the activities of $ZrSiO_4$ and $HfSiO_4$ are equal to one because pure zircon and synthetic hafnon were used in these experiments. Therefore;

$$K_{ZrSiO4} = a_{ZrO2}^{melt} \cdot a_{SiO2}^{melt}$$

$$K_{HfSiO4} = a_{HfO2}^{melt} \cdot a_{SiO2}^{melt}.$$

The activity of silica in the melt is changed by the addition of fluxing compounds as evidenced by the shift of the granite minimum composition away from the SiO_2 apex. However, given the total amount of fluxes in this study, and that an insignificant amount of SiO_2 was added to the melt by the dissolution of zircon and hafnon, a_{SiO2}^{melt} was assumed to be nearly constant. Consequently, the solubility of zircon and hafnon are reported as wt.% and mol/kg dissolved into the melt (Tables 4 and 5). Glass, zircon and hafnon crystals were the only phases observed in most experiments. However, backscattered images show that some hafnon crystals have a light gray phase in their cores. Microprobe analysis of these phases showed that they consist about 90 wt.% HfO_2 and

Table 3
Mn-tantalite solubility.

Experiments	T (C°)	P kbar	Duration (days)	ASI	EA	ASI_{Li}	EA_{Li}	ASI_{eff}	EA_{Li+P}	F wt.%	Ag_2O wt.%	MnO wt.%	Ta_2O_5 wt.%	Mn/Nb	$logK_{Sp}^{MnTa}$ $_{mol^{22}/kg}$
SO.47	700	2	5	1.10	−0.29	0.90	0.32	0.99	0.02	6	0.0 (0.1)	0.22 (0.02)	2.46 (0.15)	0.28 (0.20)	−2.75 (0.02)
Ta1	800	2	5	1.05	−0.15	0.81	0.76	0.86	0.54	0	0.0	0.52 (0.05)	2.77 (0.11)	0.58 (0.06)	−2.34 (0.06)
Ta2	800	2	5	1.05	−0.17	0.84	0.59	0.90	0.36	2	0.5 (0.11)	0.52 (0.02)	2.73 (0.06)	0.59 (0.03)	−2.34 (0.03)
Ta3	800	2	5	1.05	−0.15	0.83	0.64	0.88	0.41	4	2.0 (0.2)	0.52 (0.03)	2.55 (0.09)	0.64 (0.04)	−2.37 (0.04)
Ta4	800	2	5	1.10	−0.29	0.86	0.46	0.94	0.18	6	1.6 (0.13)	0.53 (0.03)	2.33 (0.11)	0.70 (0.05)	−2.41 (0.04)
SO.35	800	2	5	1.32	−0.89	1.06	−0.21	1.00	−0.01	6	0.0	0.22 (0.01)	1.37 (0.04)	0.50 (0.05)	−2.99 (0.04)
$SO.43^R$	800	2	5	1.05	−0.15	0.81	0.73	0.87	0.51	0	0.0	0.46 (0.01)	2.42 (0.05)	0.60 (0.01)	−2.45 (0.01)
$SO.39^R$	800	2	5	1.10	−0.29	0.87	0.44	0.95	0.14	6	0.0 (0.02)	0.46 (0.01)	2.43 (0.05)	0.60 (0.01)	−2.44 (0.01)
SO.2	1000	2	2	1.05	−0.15	0.76	0.99	0.81	0.76	0	0.0	0.97 (0.02)	6.13 (0.05)	0.49 (0.01)	−1.72 (0.01)
SO.6	1000	2	2	1.10	−0.29	0.81	0.67	0.89	0.38	6	0.2 (0.02)	0.93 (0.02)	5.87 (0.12)	0.49 (0.01)	−1.76 (0.01)

Microprobe analysis of Mn-tantalite solubility. Values in parentheses represent 2σ standard deviation. R: reverse experiments. ASI is the molar ratio of Al/(Na + K); EA is the molar Na + K–Al per kilogram; ASI_{Li} is the molar ratio of Al/(Na + K + Li + 2 ∗ Mn); EA_{Li} is the molar Na + K + Li + 2 ∗ Mn–Al per kilogram; ASI_{eff} is the molar ratio of (Al ± P)/(Na + K + Li + 2 ∗ Mn); and EA_{Li+P} is the molar Na + K + Li + 2 ∗ Mn–Al ± P per kilogram (see the text for more information about P role).

Table 4
Zircon solubility.

Experiments	T (C°)	P kbar	Duration (days)	ASI	EA	ASI_{Li}	EA_{Li}	ASI_{eff}	EA_{Li+P}	F wt.%	Ag_2O wt.%	ZrO_2 wt.%	ZrO_2 mol/kg 10^{-3}
Zr1	800	2	5	1.05	−0.15	0.87	0.50	0.93	0.28	0	0.0	0.25 (0.04)	0.20 (0.4)
Zr2	800	2	5	1.05	−0.17	0.91	0.33	0.97	0.10	2	0.5 (0.11)	0.26 (0.02)	0.24 (0.2)
Zr3	800	2	5	1.05	−0.15	0.89	0.38	0.96	0.15	4	2.0 (0.2)	0.37 (0.03)	0.30 (0.3)
Zr4	800	2	5	1.10	−0.29	0.98	0.21	1.02	−0.09	6	1.6 (0.13)	0.38 (0.03)	0.31 (0.3)
SO.26	800	2	5	1.08	−0.22	0.90	0.31	1.00	−0.02	8	6.0 (0.15)	0.47 (0.03)	0.38 (0.3)
SO.44[R]	800	2	5	1.05	−0.15	0.87	0.50	0.93	0.28	0	0.0	0.24 (0.01)	0.20 (0.1)
SO.40[R]	800	2	5	1.10	−0.29	0.98	0.21	1.02	−0.09	6	0.02 (0.01)	0.40 (0.02)	0.33 (0.2)
SO.3	1000	2	2	1.05	−0.15	0.87	0.50	0.93	0.28	0	0.0	0.65 (0.02)	0.53 (0.2)
SO.4	1000	2	2	1.10	−0.29	0.98	0.21	1.02	−0.09	6	0.17 (0.02)	0.94 (0.02)	0.28 (0.2)

Microprobe analysis of zircon solubility. Values in parentheses represent 2σ standard deviation. R: reverse experiments. ASI is the molar ratio of Al/(Na + K); EA is the molar Na + K–Al per kilogram; ASI_{Li} is the molar ratio of Al/(Na + K + Li); EA_{Li} is the molar Na + K + Li–Al per kilogram; ASI_{eff} is the molar (Al ± P)/(Na + K + Li); and EA_{Li+P} is the molar Na + K + Li–Al ± P per kilogram (see the text for more information about P role).

9.18 wt.% SiO_2, which indicates unreacted HfO_2 from the hafnon synthesis experiments. The same problem was reported by Linnen (1998) and was explained by unreacted or excess HfO_2. These are always in crystal cores, and are rare, and thus they do not affect hafnon solubility.

The glass contents of Ag_2O are reported with solubilities results (Tables 2, 3, 4 and 5). It should be noted that silver is a monovalent metal, although it has a smaller ionic radius and heavier atomic mass compared to Na^+ and K^+. The glasses used to conduct dissolution experiments in F-rich melts contain more than 1 wt.% AgO, but the crystallization experiments for F-rich compositions have negligible amounts of Ag (there are no Ag phases so it is assumed that Ag formed an alloy with the capsule material). Because the amount of Ag in the melts for the forward and reverse experiments is different, but the solubilities of HFSE minerals are similar, we conclude that Ag does not act as a network-modifier, and thus this element is not included in ASI calculations.

3.1. Temperature dependence

The temperature dependence of the logarithmic values of Mn-columbite and Mn-tantalite solubility products are shown in Figs. 2 and 3. The solubility products show linear relationships with temperature (1000/K). The solubilities products of Mn-columbite and Mn-tantalite increase from −3.23 (mol^2/kg^2) and −2.75 (mol^2/kg^2), respectively, at 700 °C, to −1.77 and −1.75, respectively, at 1000 °C. The solubility values of Mn-columbite and Mn-tantalite at 600 °C (−4.0 and −3.2(mol^2/kg^2), respectively) were extrapolated from the equation of the regression lines in Figs. 2 and 3. The data of Linnen and Keppler (1997), Linnen (1998) for 1 wt.% Li_2O (1998), Van Lichtervelde et al. (2010), for Mn-tantalite and Fiege et al. (2011) for Mn-columbite solubility, are shown for comparison. In all of the previous studies the glasses have an ASI value close to 1 except for Linnen (1998) and Van Lichtervelde et al. (2010). However, Linnen (1998) and Van Lichtervelde et al. (2010) glasses contain Li, and the ASI_{Li} values in these studies are close to 1 and 0.83, respectively. The solubility products of Mn-columbite and Mn-tantalite of this study experiments conducted at 700 °C, are plotted with the data from experiments conducted at 800 and 1000 °C, and the linear regressions of two series of experiments have R^2 values of 0.99 and 0.97, respectively. If only the data for 1000 and 800 °C are used, the values extrapolated to 700 °C are close to the 700 °C data obtained from dissolution experiments (Figs. 2 and 3), which indicate that the data from 700 °C are close to equilibrium.

The slope of the linear regression line is close to those reported by Linnen and Keppler (1997) and Linnen (1998) for subaluminous melts for both Mn-columbite and Mn-tantalite, and close to the slope reported by Van Lichtervelde et al. (2010) for Mn-tantalite. Although the glasses in this study and Van Lichtervelde et al. (2010) have ASI_{Li} 0.87 and 0.83, respectively, the slope generated from these experiments in alkaline glasses differs from the slope reported by Linnen and Keppler (1997) for peralkaline melts. That can be attributed to the presence of phosphorous in our glasses, and similarly in Van Lichtervelde et al. (2010) glasses, which shifts the ASI toward peraluminous composition (the role of phosphorous will be discussed in composition dependence). Therefore, if Li and P are included in ASI, the ASI_{Li-P} is 0.93 for our glasses and 1 for Van Lichtervelde et al. (2010), which is close to the glass ASI reported by Linnen and Keppler (1997) and Linnen (1998). By contrast, the slope reported by Fiege et al. (2011) for Mn-columbite is lower than all other slopes at a similar ASI, and even lower than the slope reported by Linnen and Keppler (1997) for peralkaline melts. However, the slope is poorly constrained because the line was generated from only two data points.

Table 5
Hafnon solubility.

Experiments	T (C°)	P kbar	Duration (days)	ASI	EA	ASI_{Li}	EA_{Li}	ASI_{eff}	EA_{Li+P}	F wt.%	Ag_2O wt.%	HfO_2 wt.%	HfO_2 mol/kg 10^{-3}
Hf1	800	2	5	1.05	−0.15	0.87	0.50	0.93	0.28	0	0.1 (0.1)	0.85 (0.05)	0.40 (0.3)
Hf2	800	2	5	1.05	−0.17	0.91	0.33	0.97	0.10	2	0.0	0.95 (0.11)	0.45 (0.7)
Hf3	800	2	5	1.05	−0.15	0.89	0.38	0.96	0.15	4	0.5 (0.11)	1.08 (0.18)	0.51 (1.2)
Hf4	800	2	5	1.10	−0.29	0.98	0.21	1.02	−0.09	6	2.0 (0.2)	1.16 (0.11)	0.55 (0.7)
SO.37	800	2	5	1.32	−0.88	1.09	−0.31	1.04	−0.12	4.7	0.0	0.37 (0.06)	0.18 (0.4)
SO.27	800	2	5	1.08	−0.22	0.90	0.31	1.00	−0.02	8	6.0 (0.15)	1.30 (0.09)	0.62 (0.6)
SO.45[R]	800	2	5	1.05	−0.15	0.87	0.50	0.93	0.28	0	0.0	0.85 (0.05)	0.40 (0.3)
SO.7	1000	2	2	1.05	−0.15	0.87	0.50	0.93	0.28	0	0.0	1.62 (0.10)	0.77 (0.6)
SO.8	1000	2	2	1.10	−0.29	0.98	0.21	1.02	−0.09	6	0.18 (0.03)	1.92 (0.08)	0.63 (0.5)

Microprobe analysis of hafnon solubility. Values in parentheses represent 2σ standard deviation. R: reverse experiments. ASI is the molar ratio of Al/(Na + K); EA is the molar Na + K–Al per kilogram; ASI_{Li} is the molar ratio of Al/(Na + K + Li); EA_{Li} is the molar Na + K + Li–Al per kilogram; ASI_{eff} is the molar ratio of (Al ± P)/(Na + K + Li); and EA_{Li+P} is the molar Na + K + Li–Al ± P per kilogram (see the text for more information about P role).

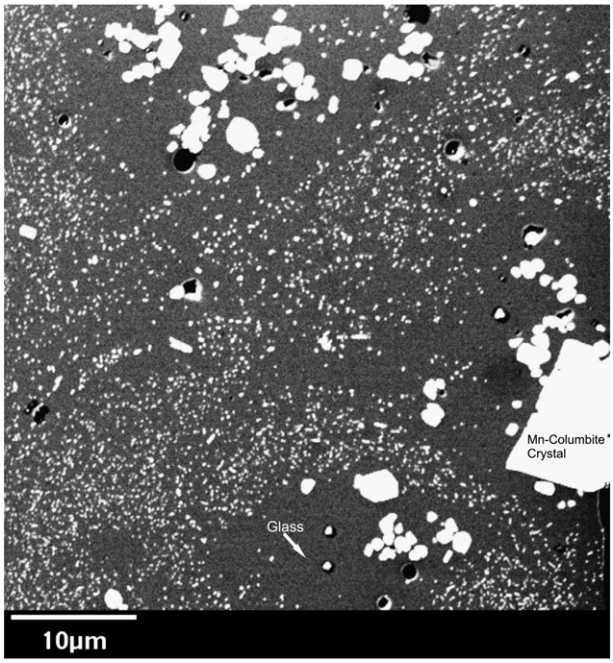

Fig. 1. Backscattered image of Mn-columbite reversal experiment (SO.43R) at 800 °C and 2 kbar. Very fine crystals formed during crystallization experiments. The crystal-free glass (gray color) around the large seed crystals (white color) were used to acquire EMP analysis.

The enthalpy of dissolution (ΔH_{diss}) of Mn-columbite and Mn-tantalite can be calculated from the slopes in Figs. 2 and 3 according to:

$$d\ln K/d(1/T) = -\Delta H_{diss}/R$$

where T is the temperature in Kelvin and R is the gas constant. Therefore, the enthalpy for Mn-columbite and Mn-tantalite are 117.1 ± 1.4 and 79.5 ± 0.7 kJ/mol, respectively. The enthalpy of Mn-columbite and Mn-tantalite of previous studies are 158 and 109 kJ/mol for Linnen and Keppler (1997), 170 and 100 kJ/mol for Linnen (1998), respectively, 79 kJ/mol for Van Lichtervelde et al. (2010), for Mn-tantalite and 31.7 kJ/mol for Fiege et al. (2011), for Mn-columbite.

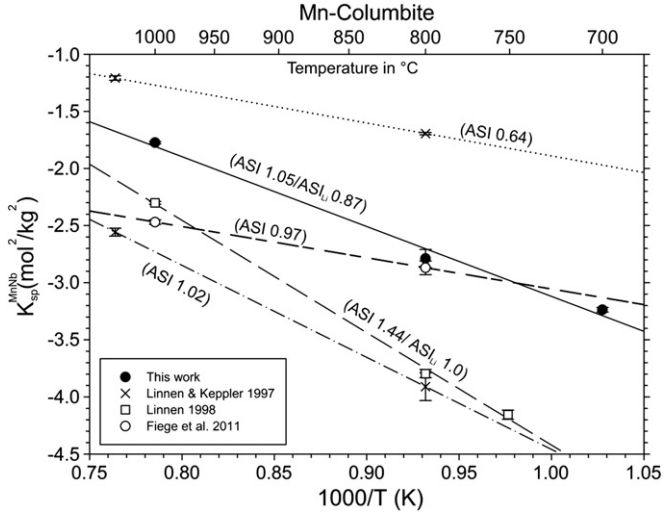

Fig. 2. Temperature dependence of Mn-columbite in water saturated haplogranitic melts at 2 kbar. This work data represents the data of the 1000 °C and 800 °C dissolution experiments and the extrapolated value of experiment at 700 °C. The previous work data were plotted here for comparison.

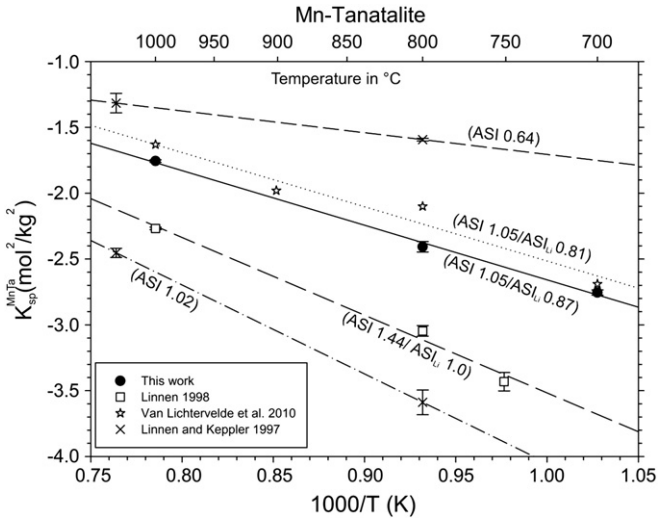

Fig. 3. Temperature dependence of Mn-tantalite in water saturated haplogranitic melts at 2 kbar. This work data represents the data of the 1000 °C and 800 °C dissolution experiments and the extrapolated value of experiment at 700 °C. The previous work data were plotted here for comparison.

These differences in enthalpy of the dissolution are potentially explained by the different ASIs of the different experimental data sets.

3.2. Fluorine dependence

3.2.1. Mn-columbite and Mn-tantalite

The solubility products of Mn-columbite and Mn-tantalite are plotted against fluorine concentration in the melt (Figs. 4 and 5). The log K_{Sp}^{MnNb} values are −2.72 ± 0.02 for the 0 wt.% F melt and −2.79 ± 0.08 for the 6 wt.% F melt (Table 2) and the log K_{Sp}^{MnTa} values are −2.34 ± 0.06 for the 0 wt.% F melt and −2.41 ± 0.04 for the 6 wt.% F melt (Table 3). Thus, within analytical error, F has no effect on the solubilities of Mn-columbite and Mn-tantalite for this melt composition, which is in agreement with Fiege et al (2011). This contradicts the results of Keppler (1993), who reported that F increases the solubilities of Mn-columbite and Mn-tantalite. According to Fiege et al (2011) the difference may be due to difficulties of reaching equilibrium in the

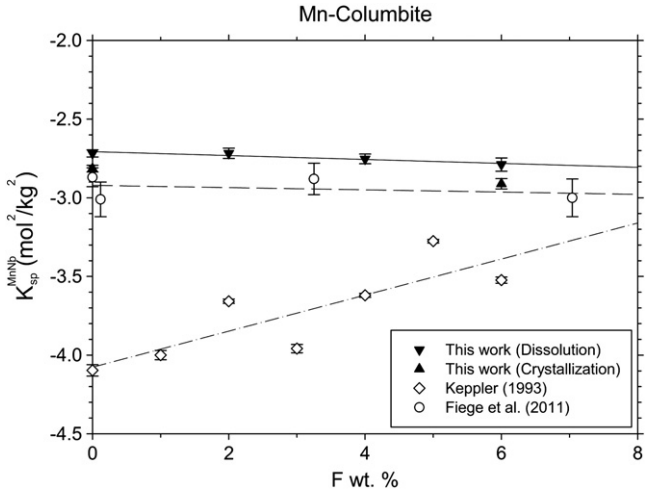

Fig. 4. Fluorine effects on the solubility of Mn-columbite. This work results show that fluorine has no effect on the solubility products of Mn-columbite which supports Fiege et al.'s (2011) conclusions. In contrast, Keppler (1993) showed that fluorine increases the solubility of Mn-columbite.

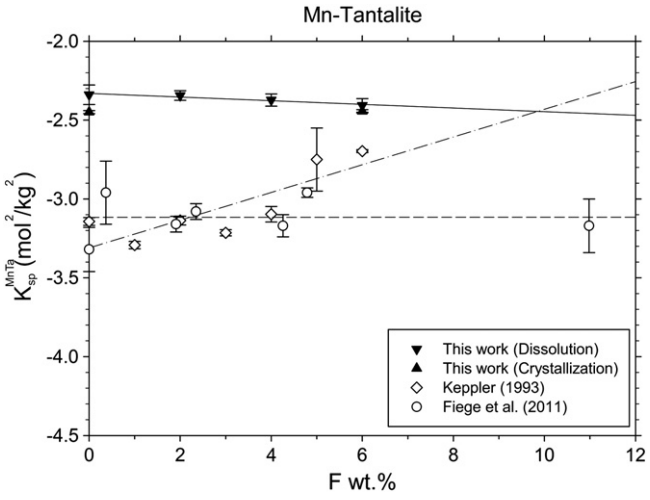

Fig. 5. Fluorine effects on the solubility of Mn-tantalite. This work results show that fluorine has no effect on the solubility products of Mn-tantalite which supports Fiege et al.'s (2011) conclusions. In contrast, Keppler (1993) showed that fluorine increases the solubility of Mn-tantalite.

experiments that were conducted at low temperature. At the equilibrium, the Mn/Nb and Mn/Ta ratios in the melt should be 0.50. However, the Keppler (1993) experiments conducted at 800 °C and 2 kbar show values larger than 0.50. Another possible reason is that the melt composition in this study contains Li, which may behave like an alkali (Van Lichtervelde et al., 2010). Thus it is possible that the differences are related to differences in the effective ASI of the melt, as discussed below.

3.2.2. Zircon and hafnon

The solubilities of zircon and hafnon are plotted against F concentration in the melt in Fig. 6. Watson (1979) reported that the solubility of zircon in water saturated haplogranitic melts (ASI = 1.0) at 800 °C and 2 kbar is less than 100 ppm of Zr. The data for this study show dramatic increases in the solubilities of zircon and hafnon from 0.25 ± 0.04 and 0.85 ± 0.05 wt.% to 0.47 ± 0.03 and 1.30 ± 0.09 wt.%, respectively, with increasing F concentration from 0 to 8 wt.%. A similar behavior of zircon was reported by Keppler (1993), who interpreted that the increased solubility as possible direct reaction between F and Zr or due to the NBO generated by the existence of F in the melt, which could form complexes with Zr. However, the saturation level of zircon in

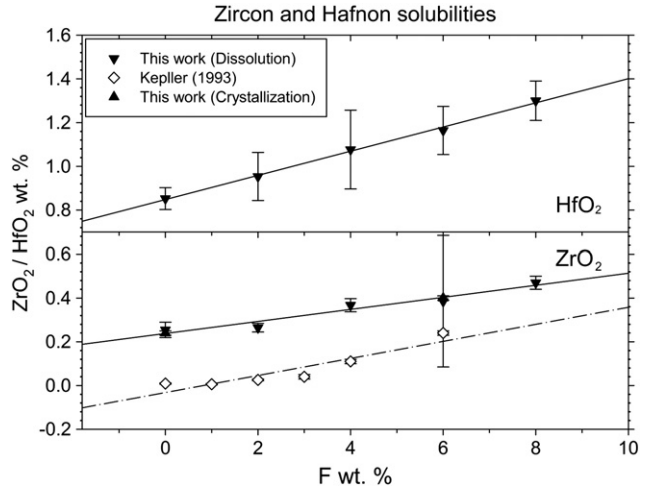

Fig. 6. Fluorine effects on the solubilities of zircon and hafnon. This work results show that solubility increases with increasing the fluorine concentration in the melt, and that supports Keppler's (1993) findings.

this study is much higher than Keppler (1993), which can be explained by the more alkaline nature of glasses in this study.

3.3. Attainment of equilibrium

In order to demonstrate an equilibrium, the experiment duration should be long enough to reach equilibrium and the Mn/Nb and Mn/Ta ratios must be constant throughout the melt at experimental conditions (Tables 2 and 3). Based on the previous studies of Linnen and Keppler (1997), Bartels et al. (2010) and Fiege et al. (2011), experiment durations between four and eight days should be sufficient to reach equilibrium. The melts in this study are flux-rich and slightly more alkaline than those of Fiege et al (2011). Therefore, the diffusivities of Nb, Ta, Zr, Hf and Mn are faster than the diffusivities of the same elements in peraluminous melts or flux-free melts. Thus, experiments with five days' duration should be long enough to reach equilibrium.

Equilibrium is best demonstrated if the values for dissolution and crystallization experiments are the same. Two glasses (0 wt.% F and 6 wt.% F) were chosen to conduct reverse (crystallization) experiments at 800 °C and 2 kbar. The results of these experiments show that the solubility values are close to those obtained from dissolution experiments, which indicates that five days is enough to reach equilibrium (Figs. 4, and 5).

4. Discussion

4.1. The role of fluorine in the melt

Fluorine has a significant role in silicate melts, e.g., to reduce the viscosity and increase the diffusivity due to depolymerization (Dingwell et al., 1985). Schaller et al. (1992) reported that F preferentially coordinates with Al to form octahedral AlF_3 in anhydrous nephleline, jadeite and albite glasses. The presence of F – Si and F – alkali bonds was reported to be unlikely based on cross-polarization/magic angle spinning and nuclear magnetic resonance spectra (Schaller et al., 1992). The decrease in viscosity with increasing F content in the melt was explained by the complexing of F with Al from bridging AlO_4, which causes depolymerization of the melts. This process will increase the amount of NBO which should increase the solubilities of HFSE in the melts. Keppler (1993) showed that increasing F content in the water-saturated haplogranitic melt increases the solubilities of rutile and zircon at 800 °C and 2 kbar in haplogranitic melts (ASI 1.0). The mechanism that was proposed is that F could react directly with HFSE and form fluorocomplexes, or could react with NBO generated by the reaction of F with bridging AlO_4.

The results from this study indicate that Mn-columbite and Mn-tantalite solubilities do not change with increasing F content in the melts, in agreement with Fiege et al. (2011). That suggests that F does not react with bridging Al to generate NBO, nor does it react with Nb and Ta. It is interesting that TaO_6Si_5Al moieties are proposed for Ta (Mayanovic et al, 2013) thus it is possible that Ta 'out competes' F for Al. Van Lichtervelde et al. (2010) also proposed an affinity of Ta for Al, based on the crystallization of simpsonite $[Al_4Ta_3(O,OH,F)_{14}]$ in some experiments. Another possible coordination of F in the silicate melts is by reacting with alkalis or Si. If F reacts with alkalis, that would decrease the solubility of Mn-columbite and Mn-tantalite. From this study, a slight decrease in solubility was observed in both Mn-columbite and Mn-tantalite experiments, which could mean that a small amount of alkalis reacts with F. However, according to Schaller et al. (1992) F-alkalis spectra were not found in his study.

The results for zircon and hafnon solubilities contrast those of Mn-columbite and Mn-tantalite. The increase of zircon and hafnon solubilities with increasing F content in the melt suggests that F may form complexes with these elements, or that Al is not part of the moiety and thus AlF_3 complexes do increase NBO. However, we do not favor increased zircon-hafnon solubilities due to an increase of NBO because the solubilities of Mn-columbite and Mn-tantalite were not observed to

increase with increasing F. Since the only difference between these experiments is the minerals that are dissolved, the increase in zircon and hafnon solubilities could be due to the direct reaction between F and Zr or Hf, but not Nb and Ta, in the melt (Keppler, 1993). However, Farges (1996) showed that F was not found as first neighbors around Zr in F-bearing albitic glass. Therefore, more analyses (X-ray absorption fine structure (XAFS) and NMR) on the melt structure are needed to show the effect of F on the solubilities of HFSE minerals and support the hypothesis of the direct coordination of F with Zr and Hf, but not Nb and Ta, in the investigated melts.

4.2. Composition dependence and the effect of fluxing elements

It is well established that the solubilities of HFSE minerals are higher in flux-rich melts (e.g., Bartels et al. 2010). What is not clear is whether or not the increase in solubility is due to a change in the effective ASI of the melt or whether there is a more direct relationship between solubility and specific fluxing compounds. In order to address this issue we have calculated the melt composition parameters in terms of an effective ASI. It is more instructive to express melt compositions in terms of excess mol/kg Al or alkalis (Na and K), because this can be directly related to the amount of NBO in the melt (Watson, 1979). The mol/kg values of Na + K–Al are reported as excess alkali (EA) in Tables 1 to 5. Where the EA value is equal to 0, the melt is metaluminous and all Na^+ and K^+ are associated with tetrahedral Al; EA values are positive in peralkaline melts and the excess alkalis act as network-modifiers that provide the melt with NBO; and negative EA values indicate that the melt is peraluminous with a deficit in alkalis to charge-balance tetrahedral Al. Lithium may also act as a network-modifier (Linnen, 1998) as can manganese, but since the latter is a divalent cation it can charge compensate two NBOs (Linnen and Keppler, 1997). If Li^+ and Mn^{2+} act as network-modifiers, the melt composition can be written as the mol/kg Na + K + Li + 2Mn–Al (reported as EA_{Li} in Tables 1 to 5).

The presence of phosphorous in silicate melts can change properties such as lowering the solidus temperatures and reducing the viscosities of the melts (e.g., Dingwell et al., 1993; London et al., 1993). Toplis and Dingwell (1996) reported that the addition of P_2O_5 in peralkaline melts increases the effective ASI (more polymerized) through the formation of alkali phosphate complexes such as Na_3PO_4, $Na_4P_2O_7$ or $NaPO_3$. (see also Mysen, 1988 and Mysen and Richet, 2005). If the addition of phosphorous in peralkaline melts decreases the number of network-modifiers, and NBO and it can be predicted that the solubilities of HFSE minerals should decrease. The stoichiometry of the phosphorous complexes in the current study is unknown, but the melts have an ASI of 1.0 if only Al/(Na + K) is considered and we assume a Na:P ratio of 1:1. Therefore, phosphorous was included in the compositional term for melts that are effectively peralkaline and the effective excess alkalis EA_{Li+P}, is the mol/kg Na + K + Li + 2Mn–Al–P value. In peraluminous melts phosphorous likely forms $AlPO_4$ complexes (Mysen, 1988; Toplis and Dingwell, 1996). This is also consistent with the increase of Raman bands associated with Si – O – Si vibrations in P-bearing glasses (Gan and Hess, 1992). Therefore, for the melt composition term for peraluminous compositions EA_{Li+P} is defined as the mol/kg Na + K + Li + 2Mn + P–Al.

The solubilities in this study are examined as a function of EA, EA_{Li} and EA_{Li+P} and compared to the solubility data obtained from flux free glasses: Linnen and Keppler (1997) for Mn-columbite and Mn-tantalite, Watson (1979) and Linnen and Keppler (2002) for zircon and Linnen and Keppler (2002), for hafnon. The solubility data in melts with variable fluorine contents suggests that Nb–Ta and Zr–Hf are complexed differently in silicate melts, thus these two pairs will be discussed separately.

4.2.1. Mn-columbite and Mn-tantalite

The solubility products of Mn-columbite and Mn-tantalite in this study were plotted in Figs. 7A and 8A and compared to the EA values

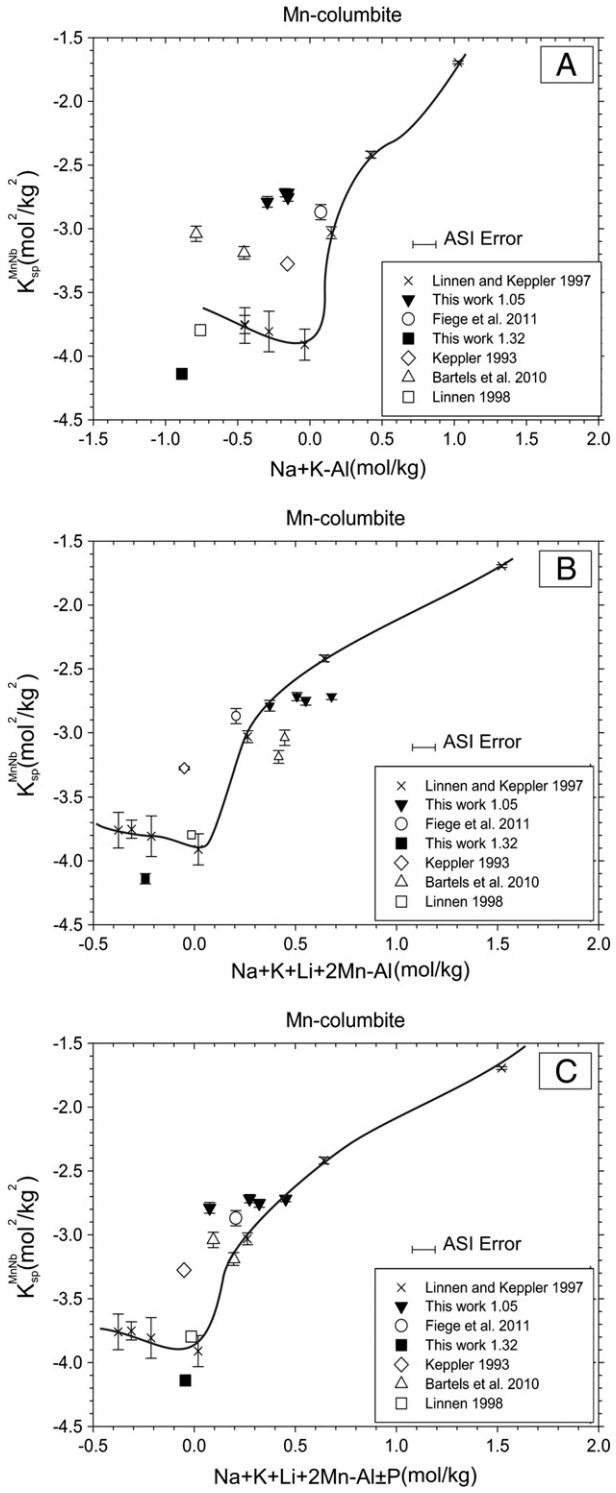

Fig. 7. The effect of melt composition on the solubility of Mn-columbite at 800 °C and 2 kbar. The data of Linnen and Keppler (1997) were plotted here for comparison. Other data points for similar melt composition were plotted as well. The values (1.05 and 1.32) of this work represent the ASI values of the glasses; however, in panels B and C the ASI was modified to include Li and P. The curve is from Linnen and Keppler (1997). The solubility products were plotted against EA in A, EA_{Li} in B and EA_{Li+P} in C (see the text for more discussion).

of previous studies. The EA value of this study is a cluster, except for the 6 wt.% F melt composition, although this point is within the analytical error of the other compositions. The K_{Sp}^{MnNb} and K_{sp}^{MnTa} values of the ASI = 1.05 series are higher than those of Linnen and Keppler (1997) at equivalent melt compositions. Similarly, Linnen (1998), Bartels

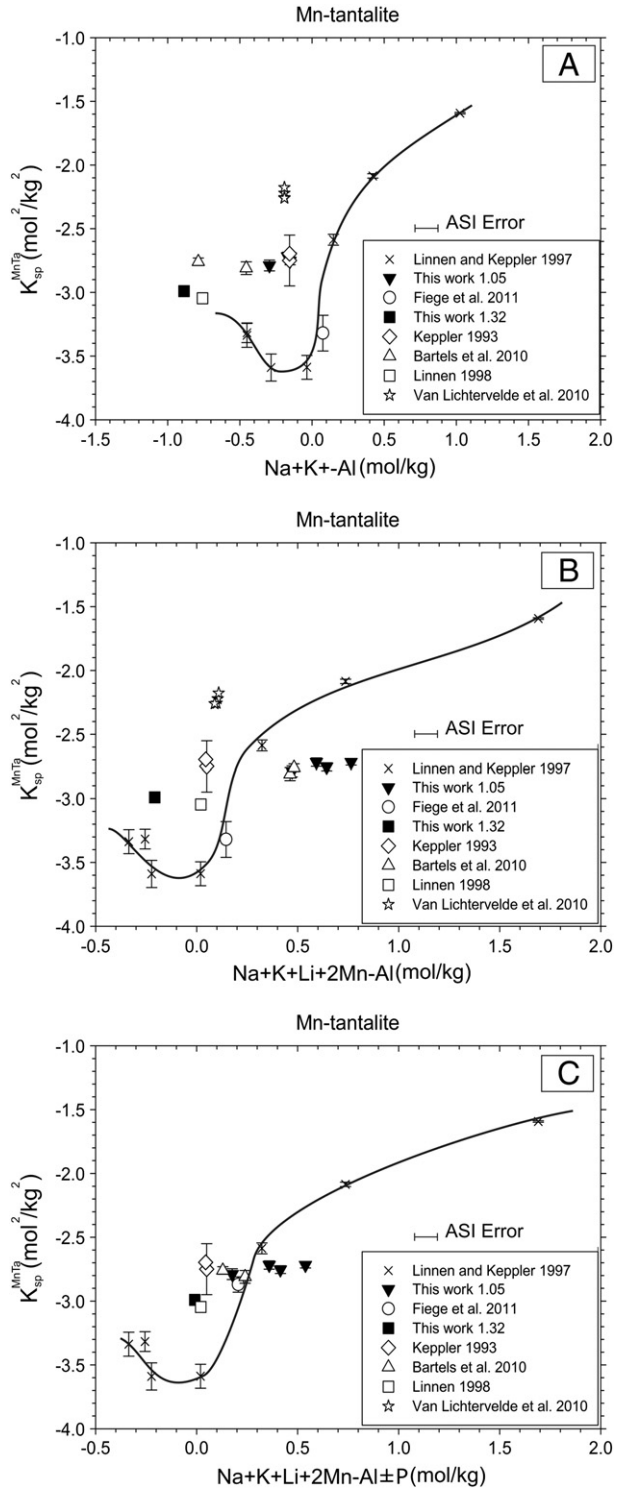

Fig. 8. The effect of melt composition on the solubility of Mn-tantalite at 800 °C and 2 kbar. The data of Linnen and Keppler (1997) were plotted here for comparison. Other data points for similar melt compositions were plotted as well. The values (1.05 and 1.32) of this work represent the ASI values of the glasses; however, in panels B and C the ASI was modified to include Li and P. The curve is from Linnen and Keppler's (1997) study. The solubility products were plotted against EA in A, EA_{Li} in B and EA_{Li+P} in C (see the text for more discussion).

et al. (2010) and Van Lichtervelde et al. (2010) reported higher K_{sp}^{MnTa} values than Linnen and Keppler (1997), whereas the data of Fiege et al. (2011) are very close to that of Linnen and Keppler (1997). The high solubility values reported in this study, by Linnen (1998), Bartels et al. (2010) and Van Lichtervelde et al. (2010), appear to be due to the high concentrations of fluxing components in the melts. Figs. 7A and 8A also show K_{Sp}^{MnNb} and K_{sp}^{MnTa} values for the peraluminous melt composition (ASI 1.32). Mn-tantalite is more soluble than Mn-columbite, similar to the results of Linnen and Keppler (1997), who explained solubility differences by the differences in the chemical bonding around Nb^{+} and Ta^{+} in subaluminous melts. Another observation is that the values of Mn-columbite and Mn-tantalite solubilities are higher than those from Linnen and Keppler (1997), which also appear to be due to the high flux contents in this study melt.

In order to evaluate whether Li^{+} and Mn^{2+} are responsible for the higher solubilities of Mn-columbite and Mn-tantalite in this study melt, the melt composition term EA_{Li} was plotted against K_{Sp}^{MnNb} and K_{sp}^{MnTa} and compared to the previous studies' solubility data (Figs 7B and 8B). In Figs. 7B and 8B, the solubility values of this work peralkaline glass (ASI_{Li} 0.87 or EA_{Li} 0.50), peraluminous glass (ASI_{Li} 1.09 or EA_{Li} −0.32) and those of Bartels et al. (2010) are lower than those from Linnen and Keppler (1997), whereas the data of Linnen (1998) and Van Lichtervelde et al. (2010) are close to or fit the Linnen and Keppler (1997) curve (Van Lichtervelde et al., 2010 is only for Ta). Therefore, the last two data points of Linnen (1998) and Van Lichtervelde et al. (2010), that fit the Linnen and Keppler (1997) curve, support the conclusion of Linnen (1998) that solubilities of Mn-columbite and Mn-tantalite increase with increasing Li concentration in the melt. However, all data that are below the reference curve contain phosphorous and B, which could decrease the Mn-columbite and Mn-tantalite solubilities. However, as it was pointed out above, it was suggested that B does not change columbite solubility (Bartels et al., 2010; Wolf and London, 1993).

Figs. 7C and 8C show K_{Sp}^{MnNb} and K_{sp}^{MnTa} values plotted against EA_{Li+P}. By expressing the melt composition as EA_{Li+P}, most of the previous solubility product data are close or fit the reference curve of Linnen and Keppler (1997), i.e., that phosphorous apparently decreases the solubilities of Mn-columbite and Mn-tantalite by lowering the effective alkali content of the melt. In peraluminous melts, phosphorous decreases the tetrahedral Al in the melt, i.e., the EA_{Li+P}, value is higher than the EA_{Li} value. The values of this study are very close to those of the Linnen and Keppler (1997) curve, which we interpret to mean that phosphorous affects the solubilities of Mn-columbite and Mn-tantalite in subaluminous melts primarily by changing the effective excess alkalis rather than direct complexing. However, Wolf and London (1993) reported that for a peraluminous melt composition the solubilities of Mn-columbite and Mn-tantalite, increase with phosphorous, which is not predicted by the EA_{Li+P} model. Thus further systematic studies focusing on the effects of phosphorous on the solubilities of Mn-columbite and Mn-tantalite at different ASI are needed.

4.2.2. Zircon and hafnon

In order to investigate whether the fluxed elements in the melt have an effect on zircon and hafnon solubilities, the results of F-free experiments of this study were plotted against EA, and compared to fluxed free glasses of Watson (1979) and Linnen and Keppler (2002), as well as the study of Linnen (for hafnon, 1998) in Li-free to Li-rich glasses (Figs. 9A and 10A). The results of this study are higher than those of Watson (1979) and Linnen and Keppler (2002) (Fig. 9A), and also higher than those of Linnen (1998) for the glass that contains 1 wt.% Li_2O (Fig. 10A) if the ASI is considered to be equal to the molar Al–Na–K per kilogram. Again these higher values could be related to the contents of fluxes in these melts. Therefore, the solubilities of zircon and hafnon were plotted against EA_{Li} (Figs. 9B and 10B). Using this melt composition parameter, zircon and hafnon solubilities are below the curve of Watson (1979) and Linnen and Keppler (2002), which suggests that either Li is not acting as a network modifier or the presence of Li in the melt decreases the solubilities of zircon and hafnon. Linnen (1998) reported that the solubilities of zircon and hafnon decrease with the Li_2O concentration in the melt and proposed that the competition of Zr^{4+} and Hf^{4+} for the NBO related to Li is more difficult compared to

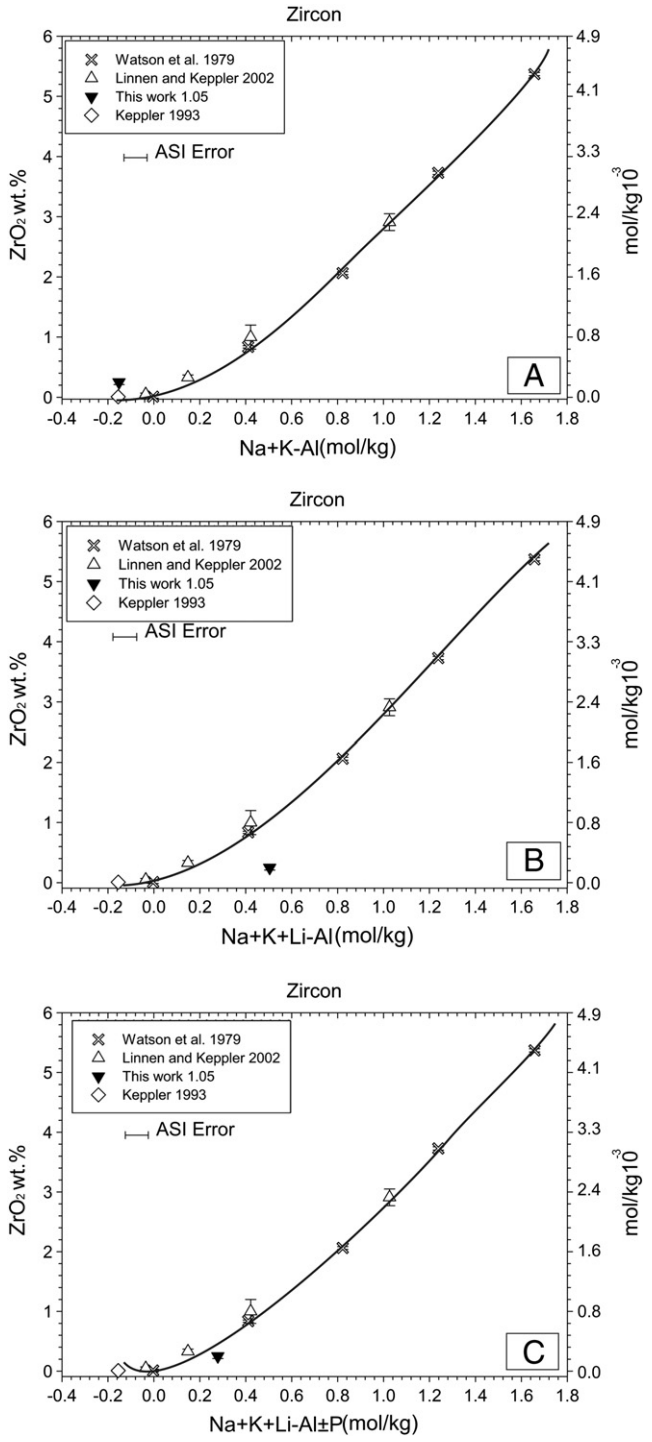

Fig. 9. Comparison of zircon solubility of this work (ASI = 1.05) to the previous studies. The curve is from Watson (1979). The solubility products were plotted against EA in A, EA_{Li} in B and EA_{Li+P} in C.

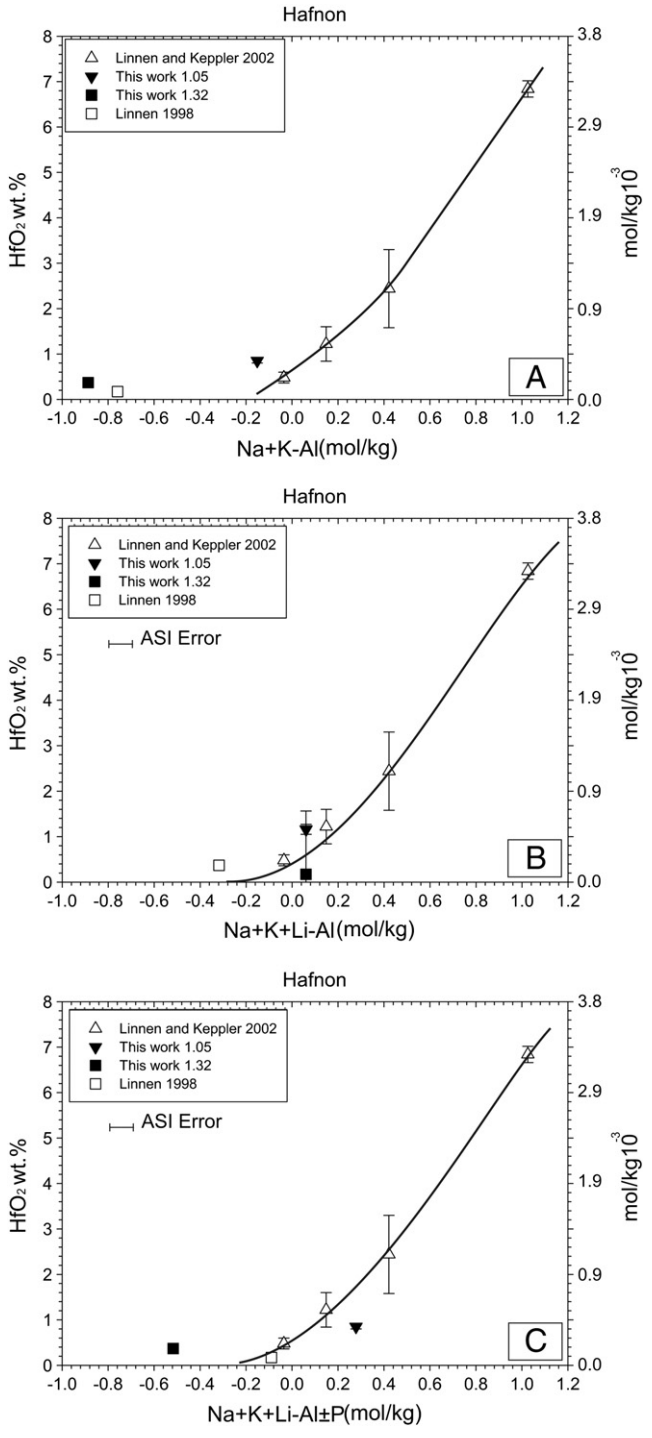

Fig. 10. Comparison of hafnon solubility of this work to the previous studies. The solubility products were plotted against EA in A, EA_{Li} in B and EA_{Li+P} in C.

other alkalis, whereas it is easier in the case of Nb^{5+} and Ta^{5+} due to the high charge and smaller ionic radius.

The effect of phosphorous on the solubilities of zircon and hafnon are shown in Figs. 9C and 10C. The solubilities were plotted against EA_{Li+P}. The comparison shows that both zircon and hafnon solubilities are close to the reference curve of Watson (1979), which suggests that the effect of phosphorous on the solubilities of zircon and hafnon can largely be accounted for by changes in the effective ASI.

In peraluminous melts, the data shows that hafnon is less soluble than its solubility in peralkaline melts. However, the results in this study show that hafnon solubility is higher than the solubility obtained by Linnen (1998) at $ASI_{Li} = 1.04$, even with the negative effect of Li on hafnon solubility (Fig. 10). This high value can be attributed to the presence of about 4 wt.% F. However, it is difficult to interpret the effect of Li and other flux components because of the complex composition of the peraluminous melt and the variation of the fluxed contents between glasses of this study and the glasses of the previous studies. Experiments that examine the roles of individual fluxing elements in silicate melts are needed to better interpret solubilities in complex systems.

5. Conclusions and implications for natural systems

This study shows that solubilities of Mn-columbite and Mn-tantalite, at experimental conditions of this study, are nearly independent of the F content of the melt, in contrast to the solubilities of zircon and hafnon which do increase with the F content of the melt. We also conclude that the effective melt ASI and temperature are the two dominant controls of Mn-columbite, Mn-tantalite, zircon and hafnon solubility similar to the control of other pegmatite minerals (cf. London, 2008). The presence of Li in the melt appears to increase the solubilities of Mn-columbite and Mn-tantalite, whereas Li decreases the solubilities of zircon and hafnon, in support of Linnen (1998).

The roles of P and B in the silicate melt and their effects on the solubilities of investigated minerals are not clear. However, the solubility data imply that phosphorous decreases the solubilities of all investigated minerals in peralkaline melt ($ASI_{Li} = 0.87$) by reacting with alkalis in the melt structure, which decreases NBO. It is difficult to predict the role of phosphorous in subaluminous melts where phosphorous could either react with alkalis and forms complexes with the alkalis, or with Al to form $AlPO_4$ complexes (Toplis and Dingwell, 1996).

Van Lichtervelde et al. (2007) showed that zircon accessory phases are associated with Ta mineralization and some zircon crystals contain inclusions of Ta oxides. This shows that zircon and Ta oxide crystallized from the same melt at the same time. Therefore, similar processes lead to Nb and Ta oxides crystallization and zircon and hafnon saturation. However, this study shows that some of factors that affect zircon and hafnon solubilities (Li and F contents in the melt) do not have the same effects on Mn-columbite and Mn-tantalite. The factors that do have the same effect on the solubilities of columbite–tantalite and zircon–hafnon are temperature and the melt ASI. Decreasing the alkali content or increasing the Al content in the melt leads to a decrease in the solubilities of all investigated minerals. Thus, if a melt undergoes alkali loss (e.g., via diffusion, volatile saturation or magmatic metasomatism, cf. Bartels et al., 2010; London, 2008; Van Lichtervelde et al. 2007), it could trigger both columbite–tantalite and zircon–hafnon crystallization.

Acknowledgments

We gratefully acknowledge a scholarship from King Abdul Aziz University to Abdullah Aseri and a NSERC Discovery Grant to Robert Linnen for supporting this research. Our thanks are also extended to Iain Samson, Melissa Price and Mohamed Shaheen for LA-ICP/MS analysis and Yanan Liu for EMP analysis. Our gratitude is also extended to Jean-Louis Vigneresse and an anonymous reviewer for their comments and suggestions.

References

Badanina, E.V., Syritso, L.F., Volkova, E.V., Thomas, R., Trumbull, R.B., 2010. Composition of Li–F granite melt and its evolution during the formation of the ore-bearing Orlovka Massif in Eastern Transbaikalia. Petrology 18, 131–157.

Baker, D.R., Conte, A.M., Freda, C., Ottolini, L., 2002. The effect of halogens on Zr diffusion and zircon dissolution in hydrous metaluminous granitic melts. Contrib. Mineral. Petrol. 142, 666–678.

Bartels, A., Holtz, F., Linnen, R.L., 2010. Solubility of manganotantalite and manganocolumbite in pegmatitic melts. Am. Mineral. 95, 537–544.

Borisova, A.Y., Thomas, R., Salvi, S., Candaudap, F., Lanzanova, A., Chmeleff, J., 2012. Tin and associated metal and metalloid geochemistry by femtosecond LA-ICP-QMS microanalysis of pegmatite–leucogranite melt and fluid inclusions: new evidence for melt–melt–fluid immiscibility. Mineral. Mag. 76, 91–113.

Breiter, K., Škoda, R., Uher, P., 2007. Nb–Ta–Ti–W–Sn–oxide minerals as indicators of a peraluminous P- and F-rich granitic system evolution: Podlesí, Czech Republic. Mineral. Petrol. 91, 225–248.

Černý, P., Ercit, T.S., Hawthorne, F.C., 2005. The classification of granitic pegmatites revisited. Can. Mineral. 43, 2005–2026.

Chevychelov, V.Yu., Borodulin, G.P., Zaraisky, G.P., 2010. Solubility of columbite, (Mn, Fe)(Nb, Ta)$_2O_6$, in granitoid and alkaline melts at 650–850 °C and 30–400 MPa: an experimental investigation. Geochem. Int. 48, 456–464.

Dingwell, D.B., Scarfe, C.M., Cronin, D.J., 1985. The effect of fluorine on viscosities in the system Na_2O–Al_2O_3–SiO_2; implications for phonolites, trachytes and rhyolites. Am. Mineral. 70, 80–87.

Dingwell, D.B., Knoche, R., Webb, S.L., 1993. The effect of P_2O_5 on the viscosity of haplogranitic liquid. Eur. J. Mineral. 5, 133–140.

Farges, F., 1996. Does Zr–F "complexation" occur in magmas? Chem. Geol. 127, 253–268.

Fiege, A., Kirchner, C., Holtz, F., Linnen, R.L., Dziony, W., 2011. Influence of fluorine on the solubility of manganotantalite ($MnTa_2O_6$) and manganocolumbite ($MnNb_2O_6$) in granitic melts; an experimental study. Lithos 122, 165–174.

Gan, H., Hess, P.C., 1992. Phosphate speciation in potassium aluminosilicate glasses. Am. Mineral. 77, 495–506.

Keppler, H., 1993. Influence of fluorine on the enrichment of high field strength trace elements in granitic rocks. Contrib. Mineral. Petrol. 114, 479–488.

Linnen, R.L., 1998. The solubility of Nb–Ta–Zr–Hf–W in granitic melts with Li and Li + F; constraints for mineralization in rare metal granites and pegmatites. Econ. Geol. 93, 1013–1025.

Linnen, R.L., 2005. The effect of water on accessory phase solubility in subaluminous and peralkaline granitic melts. Lithos 80, 267–280.

Linnen, R.L., Cuney, M., 2005. Granite-related rare-element deposits and experimental constraints on Ta–Nb–W–Sn–Zr–Hf mineralization. Short Course Notes — Geological Association of Canada, 17 pp. 45–68.

Linnen, R.L., Keppler, H., 1997. Columbite solubility in granitic melts; consequences for the enrichment and fractionation of Nb and Ta in the Earth's crust. Contrib. Mineral. Petrol. 128, 213–227.

Linnen, R.L., Keppler, H., 2002. Melt composition control of Zr/Hf fractionation in magmatic processes. Geochim. Cosmochim. Acta 66, 3293–3301.

Linnen, R.L., Samson, I.M., Williams-Jones, A.E., Chakmouradian, A.R., 2014. In: Scott, S.D. (Ed.), Geochemistry of Rare-Earth Element, Nb, Ta, Hf and Zr Deposits, 2nd ed. Treatise on Geochemistry, 13, pp. 543–568.

London, D., 1987. Internal differentiation of rare-element pegmatites; effects of boron, phosphorus, and fluorine. Geochim. Cosmochim. Acta 51, 403–420.

London, D., 2008. Pegmatites. Mineralogical Association of Canada Special Publication, 10 (347 pp.).

London, D., Morgan, G.B., Babb, H.A., Loomis, J.L., 1993. Behavior and effects of phosphorus in the system Na_2O–K_2O–Al_2O_3–SiO_2–P_2O_5–H_2O at 200 MPa (H_2O). Contrib. Mineral. Petrol. 113, 450–465.

Mayanovic, R.A., Yan, H., Anderson, A.J., Solferino, G., 2013. Investigation of the structural environment of Ta in a silicate glass and water system under high P–T conditions. J. Non-Cryst. Solids 368, 71–78.

Mysen, B.O., 1988. Structure and properties of silicate melts. Developments in Geochemistry, 4. Elsevier, Amsterdam (354 pp.).

Mysen, B.O., Richet, P., 2005. Silicate glasses and melts; properties and structure. Developments in Geochemistry. , 10. Elsevier, Amsterdam (544 pp.).

Raimbault, L., Burnol, L., 1998. The Richemont rhyolite dyke, Massif Central, France: a subvolcanic equivalent of rare-metal granites. Can. Mineral. 36, 265–282.

Schaller, T., Dingwell, D.B., Keppler, H., Knoller, W., Merwin, L., Sebald, A., 1992. Fluorine in silicate glasses: a multinuclear nuclear magnetic resonance study. Geochim. Cosmochim. Acta 56, 701–707.

Thomas, R., Webster, J.D., Heinrich, W., 2000. Melt inclusions in pegmatite quartz; complete miscibility between silicate melts and hydrous fluids at low pressure. Contrib. Mineral. Petrol. 139, 394–401.

Thomas, R., Davidson, P., Beurlen, H., 2011. Tantalite-(Mn) from the Borborema Pegmatite Province, northeastern Brazil: conditions of formation and melt and fluid-inclusion constraints on experimental studies. Mineral. Deposita 46, 749–759.

Toplis, M.J., Dingwell, D.B., 1996. The variable influence of P_2O_5 on the viscosity of melts of differing alkali/aluminium ratio; implications for the structural role of phosphorus in silicate melts. Geochim. Cosmochim. Acta 60, 4107–4121.

Van Lichtervelde, M., Salvi, S., Beziat, D., Linnen, R.L., 2007. Textural features and chemical evolution in tantalum oxides; magmatic versus hydrothermal origins for Ta mineralization in the Tanco lower pegmatite, Manitoba, Canada. Econ. Geol. 102, 257–276.

Van Lichtervelde, M., Holtz, F., Hanchar, J.M., 2010. Solubility of manganotantalite, zircon and hafnon in highly fluxed peralkaline to peraluminous pegmatitic melts. Contrib. Mineral. Petrol. 160, 17–32.

Watson, E.B., 1979. Zircon saturation in felsic liquids; experimental results and applications to trace element geochemistry. Contrib. Mineral. Petrol. 70, 407–419.

Webster, J.D., Thomas, R., Rhede, D., Foerster, H., Seltmann, R., 1997. Melt inclusions in quartz from an evolved peraluminous pegmatite; geochemical evidence for strong tin enrichment in fluorine-rich and phosphorus-rich residual liquids. Geochim. Cosmochim. Acta 61, 2589–2604.

Wise, M.A., Francis, C.A., Černý, P., 2012. Compositional and structural variations in columbite-group minerals from granitic pegmatites of the Brunswick and Oxford fields, Maine: differential trends in F-poor and F-rich environments. Can. Mineral. 50, 1515–1530.

Wolf, M.B., London, D., 1993. Preliminary results of HFS and RE element solubility experiments in "granites" as a function of B and P. EOS Trans. Am. Geophys. Union 74, 343.